Tuning of the spin gap transition of spin dimer compound $Ba_3Mn_2O_8$ by doping with La and V

2009 J. Phys.: Condens. Matter 21 236005

(http://iopscience.iop.org/0953-8984/21/23/236005)

J. Phys.: Condens. Matter **21** (2009) 236005 (6pp) doi:10.1088/0953-8984/21/23/236005

Tuning of the spin gap transition of spin dimer compound $Ba_3Mn_2O_8$ by doping with La and V

S Manna[1,2], S Majumder[2,3] and S K De[1,2,4]

[1] Department of Materials Science, Indian Association for the Cultivation of Science, Jadavpur, Kolkata 700 032, India
[2] Centre for Advanced Materials, Indian Association for the Cultivation of Science, Jadavpur, Kolkata 700 032, India
[3] Department of Solid State Physics, Indian Association for the Cultivation of Science, Jadavpur, Kolkata 700 032, India

E-mail: msskd@mahendra.iacs.res.in (S K De)

Received 12 December 2008, in final form 1 April 2009
Published 11 May 2009
Online at stacks.iop.org/JPhysCM/21/236005

Abstract

We have successfully synthesized the coupled spin dimer systems $La_xBa_{3-x}Mn_2O_8$ ($x = 0$, 0.2, 0.5, 1) and $Ba_3Mn_{2-y}V_yO_8$ ($y = 0.5$, 1.0, 2.0). The magnetic properties have been investigated as a function of magnetic field and temperature down to 2 K. The susceptibility increases and the intradimer spin exchange interaction decreases with increase of La concentration. The most important finding in higher La doped systems reveals hysteresis in magnetization as a function of magnetic field. The substitution of La ($x = 0.5$, 1.0) for Ba induces ferromagnetism due to the formation of a mixed valence state of Mn and enhancement of the inter-bilayer ferromagnetic interaction. The replacement of Mn by non-magnetic V destroys the spin gap. La and V doping significantly affect the magnetic properties of the quantum antiferromagnetic compound $Ba_3Mn_2O_8$.

1. Introduction

Quantum antiferromagnets exhibit a rich variety of novel phenomena due to complex crystalline structure, lattice topology and competing magnetic exchange interactions among neighboring spins. Short ranged spin–spin correlations in some antiferromagnetic compounds leads to a gap in the spin excitation spectrum. Low-dimensional quantum spin systems such as spin Peierls [1], spin ladder [2], frustrated spin [3, 4] and Haldane [5] mainly exhibit a spin gap between the spin singlet ground state and the excited triplet state. Particular crystalline networks in some magnetic compounds assist the formation of antiferromagnetically coupled spin dimers which reveal a gap [6, 7]. A divalent Cu ion in a $TlCuCl_3$ system [8–10] and a $BaCuSi_2O_6$ quasi-two-dimensional compound [11, 12] forms the spin dimer singlet ground state separated by the spin triplet excited state. Recently, it has been observed that the magnetic susceptibility of the series $A_3M_2O_8$ (A = Ba, Sr and M = Cr, Mn) with a three-dimensional network of isolated MO_4 tetrahedra has the characteristic behavior of a spin gap system [13, 14]. Spin dimer systems $Ba_3Cr_2O_8$ and $Sr_3Cr_2O_8$ have an excitation gap of 16 K and 62 K respectively [14, 15].

The compound $Ba_3Mn_2O_8$ is a promising spin dimer antiferromagnet which shows magnetization plateaus in high magnetic fields [16]. Specific heat measurements [17] indicate magnetic phases consistent with the magnetization plateaus. Stone *et al* [18] directly observed the spin gap and its temperature dependence by a powder inelastic neutron scattering experiment. Uchida *et al* [16] analyzed the magnetization process in the framework of the mean field approximation and found that the third nearest neighbor interdimer exchange interactions are essential to describe the magnetization process of $Ba_3Mn_2O_8$. The quantum phase transitions of this compound have also been studied by bond operator theory under the mean field approximation [19]. In $Ba_3Mn_2O_8$, the valence state of the Mn ion is Mn^{5+} and total spin $S = 1$. This compound has a trigonal unit cell (space group $R\bar{3}m$) in which all Mn ions are located at

[4] Author to whom any correspondence should be addressed.

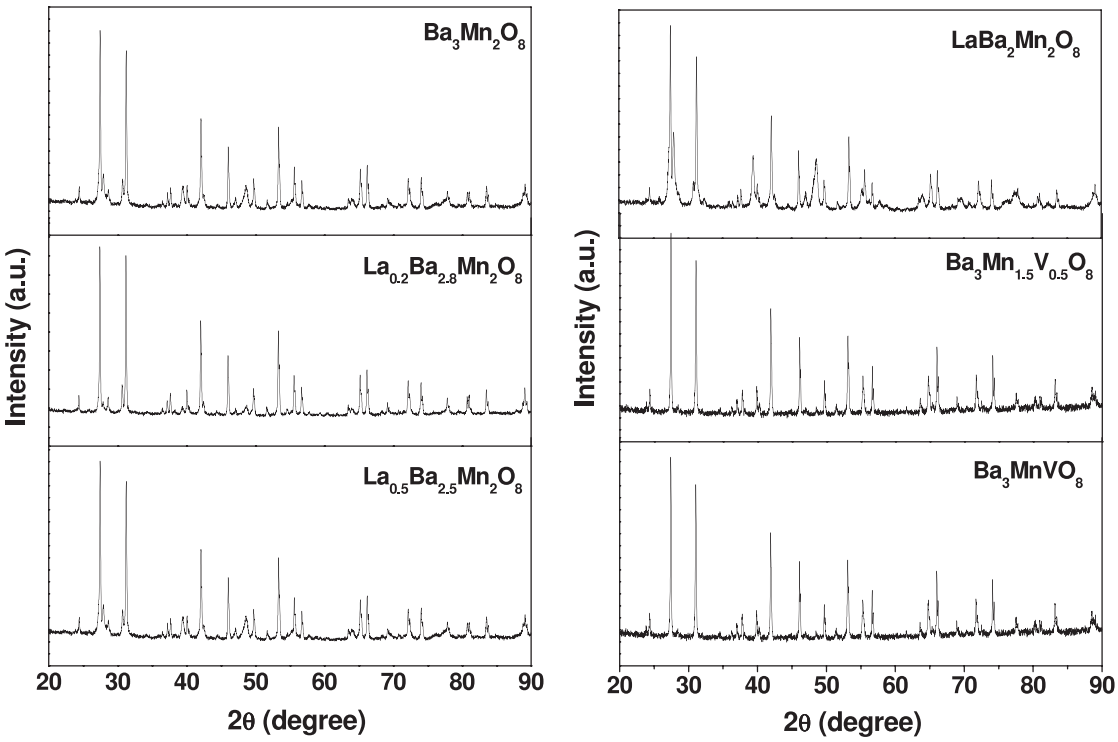

Figure 1. X-ray diffraction pattern for $La_xBa_{3-x}Mn_2O_8$ ($x = 0, 0.2, 0.5, 1$) and $Ba_3Mn_{2-y}V_yO_8$ ($y = 0.5, 1.0$).

crystallographically equivalent sites. The structure consists of two different Ba–O polyhedra, 10-coordinate and 12-coordinate [20]. Two types of Ba–O polyhedra alternate along the *c*-axis and the unit cell is composed of 3 f.u. Each Mn ion with $3d^2$ configuration is tetrahedrally surrounded by O^{2-} ions. The nearest neighbor Mn ions along the *c*-axis form dimers through antiferromagnetic interaction. The dimers are coupled through edge sharing triangular lattices in the basal plane. Stone *et al* [21] experimentally verified that inter-bilayer exchange interactions play important roles in understanding the quantum critical phase diagram and singlet–triplet dispersion of $Ba_3Mn_2O_8$. The effect of impurities on the spin dimer $Ba_3Mn_2O_8$ system has not yet been investigated. The formation as well as the stability of spin dimers primarily depend on the valence state of the magnetic ion Mn. Substitution of divalent Ba^{2+} by trivalent ions modifies the valence state of the Mn ion. Moreover the replacement of Mn by another non-magnetic transition metal also influences the magnetic ground state. In this work we have used bulk magnetic measurements of La and V doped $Ba_3Mn_2O_8$ to investigate systematically the spin gap transition.

2. Experimental details

Pure and doped $Ba_3Mn_2O_8$ materials were synthesized by solid state reaction. $BaCO_3$, MnO_2, La_2O_3, V_2O_5 are the starting raw materials. Stoichiometric amounts of these powders were mixed and ground to a very fine powder, which was then baked at 800 °C for 24 h. The reground mixture was then pressed into pellets at high pressure (5 tons). The final pellet was sintered again at 1200 °C for 30 h at atmospheric pressure. To obtain a high purity oxide the same process was repeated several times, and the total sintering time was more than 140 h. Samples with different compositions $La_xBa_{3-x}Mn_2O_8$ ($x = 0, 0.2, 0.5, 1$) and $Ba_3Mn_{2-y}V_yO_8$ ($y = 0.5, 1.0, 2.0$) were prepared to study the influence of La and V doping on the magnetic properties of $Ba_3Mn_2O_8$.

X-ray diffraction patterns of the samples were recorded with a high resolution X'Pert PRO Panalytical x-ray diffractometer. The x-ray powder diffraction patterns of all samples are shown in figure 1. All the characteristic peaks correspond to space group $R\bar{3}m$ except for some discrepancies due to the presence of some minor impurity phases in doped compounds. The modifications in the vicinity of 28° for La doped samples originate from cubic BaO and $BaMn_2O_8$ phases. The weak peak at about 35° arises from the rhombohedral phase. The small changes around 40° and 48° for La doped material are due to the formation of impurity phases such as La_2O_3, MnO_2 and Mn_3O_4. The peaks around 48° and 56° for V doped samples originate from impurity $BaMn_2V_2O_8$ and $BaMnV_2O_7$ compounds. The temperature and magnetic field dependent magnetic properties were studied with a Quantum Design SQUID magnetometer, MPMS, XL (Evercool model). High field magnetization was measured using a cryogen free low temperature and high field system (Cryogenic Ltd UK).

3. Results and discussion

Magnetization (M) of all the samples has been studied by varying both magnetic field (H) and temperature (T). The temperature dependences of susceptibility $\chi(T) = M(H)/H$

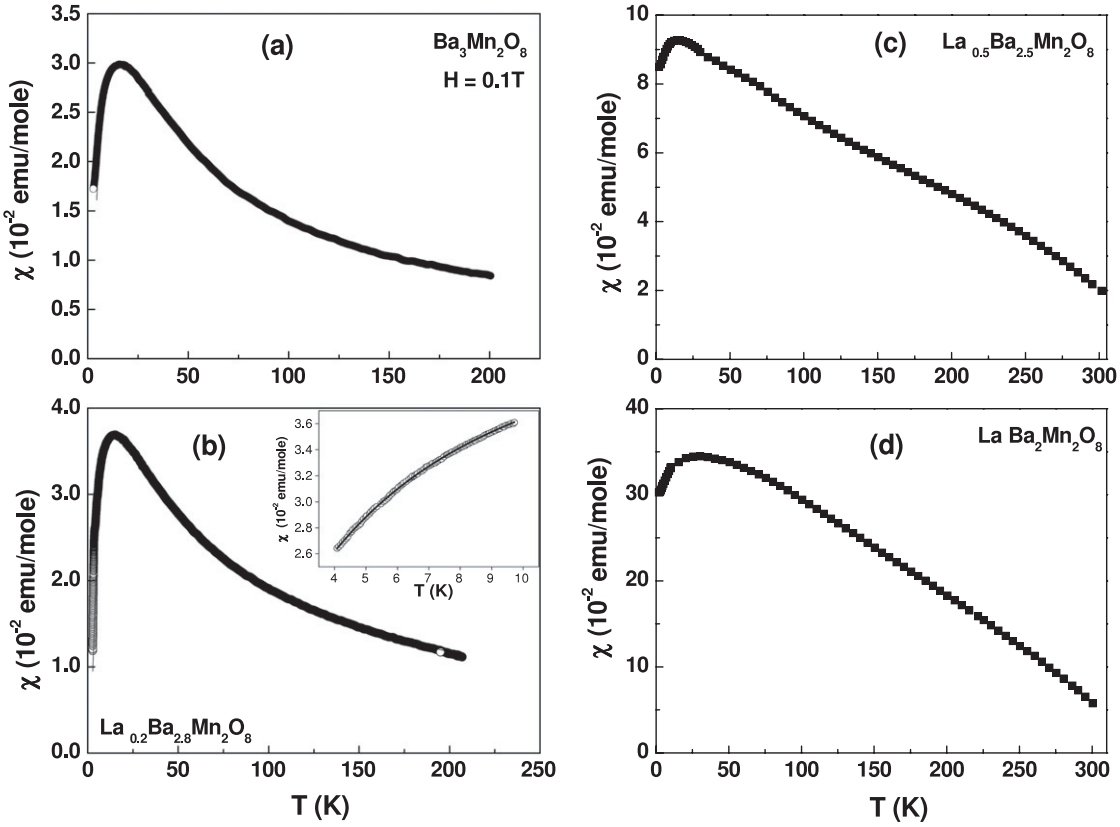

Figure 2. Temperature dependence of magnetic susceptibility for $La_xBa_{3-x}Mn_2O_8$ ($x = 0, 0.2, 0.5, 1$) measured under 0.1 T. The open circles and solid line show raw and fitted data, respectively. The inset of figure 2(b) shows the low temperature susceptibility.

at low magnetic field for $x = 0.0, 0.2, 0.5$ and 1.0 are shown in figure 2. The variation of $\chi(T)$ with temperature for $x = 0.0$ (figure 2(a)) and 0.2 (figure 2(b)) reveals a well pronounced maximum and a rapid decrease at low temperature. Such a kind of behavior of $\chi(T)$ is characteristic of a spin gap system. The $\chi(T)$ is fitted with the Curie–Weiss law, $\chi(T) = C/(T - \theta)$ at a higher temperature region than the spin gap transition. The best fitted Weiss temperatures are -10.88 K and -6.49 K for $x = 0$ and 0.2. The effective (p_{eff}) moment is determined from the values of $C = Np_{\text{eff}}^2\mu_B^2/(3k_B)$, where N is the Avogadro number, μ_B is the Bohr magneton and k_B is the Boltzmann constant. The calculated values of p_{eff} are 2.86 μ_B/Mn and 3.47 μ_B/Mn for $x = 0$ and 0.2 respectively. The theoretical value of $p_{\text{eff}} = g\sqrt{S(S+1)}\mu_B$ where we assume $g = 2$ and $S = 1$ for Mn^{5+} is 2.82 μ_B. The experimental value of p_{eff} for $x = 0$ is consistent with the Mn^{5+} configuration. The calculated value of p_{eff} for $x = 0.2$ is higher than the theoretical value. This clearly indicates the presence of a different valence state of Mn rather than Mn^{5+}.

The $\chi(T)$ for $x = 0.5$ (figure 2(c)) and 1.0 (figure 2(d)) compositions exhibits a peak at low temperature similar to a spin gap system. The maximum value of χ_{max} for the highest concentration of La ($x = 1.0$) is 34.38 emu mol^{-1} at about $T = 25$ K. The value of χ_{max} is about one order of magnitude higher than the pure compound. The behavior of $\chi(T)$ at high temperature is quite different from other systems with $x = 0$ and 0.2. The molar susceptibility increases and the $\chi(T)$ peak becomes broader with the increase of La concentration. The rounded peak and slow decrease in $\chi(T)$ for higher concentration of La indicate the suppression of the gap in the magnetic excitation spectrum. The samples for $x = 0.5$ and 1.0 do not follow the Curie–Weiss law at high temperature.

In the case of two level systems such as a singlet ground state and triplet excited state in a spin dimer, the susceptibility $\chi(T) \propto e^{-\Delta/k_BT}$, where Δ is the spin gap energy. Thus $\chi(T)$ approaches zero at low temperature. The value of Δ is estimated by fitting $\chi(T)$ below the spin gap transition temperature as shown in the inset of figure 2(b). The calculated gap Δ is 2.05 K and 4.59 K for $x = 0$ and 0.2 respectively. The separation between the singlet ground state and the triplet excited state increases with doping of the La ion.

The unusual behavior of $\chi(T)$ is generally described by considering pairwise antiferromagnetic interaction. The temperature dependence of susceptibility has been analyzed by the isolated spin ($S = 1$) dimer model [22] where the spin susceptibility is given by

$$\chi_0 = \frac{2N\beta g^2\mu_B^2(1 + 5e^{-4\beta J_0})}{3 + e^{2\beta J_0} + 5e^{-4\beta/J_0}}. \quad (1)$$

Here N is the number of the dimer, $\beta = 1/k_BT$ and J_0 is the first nearest neighbor exchange constant. It has been found that $\chi(T)$ cannot be fitted using equation (1). This implies that interactions among dimers play important roles to determine the magnetic properties. Taking into account the interdimer

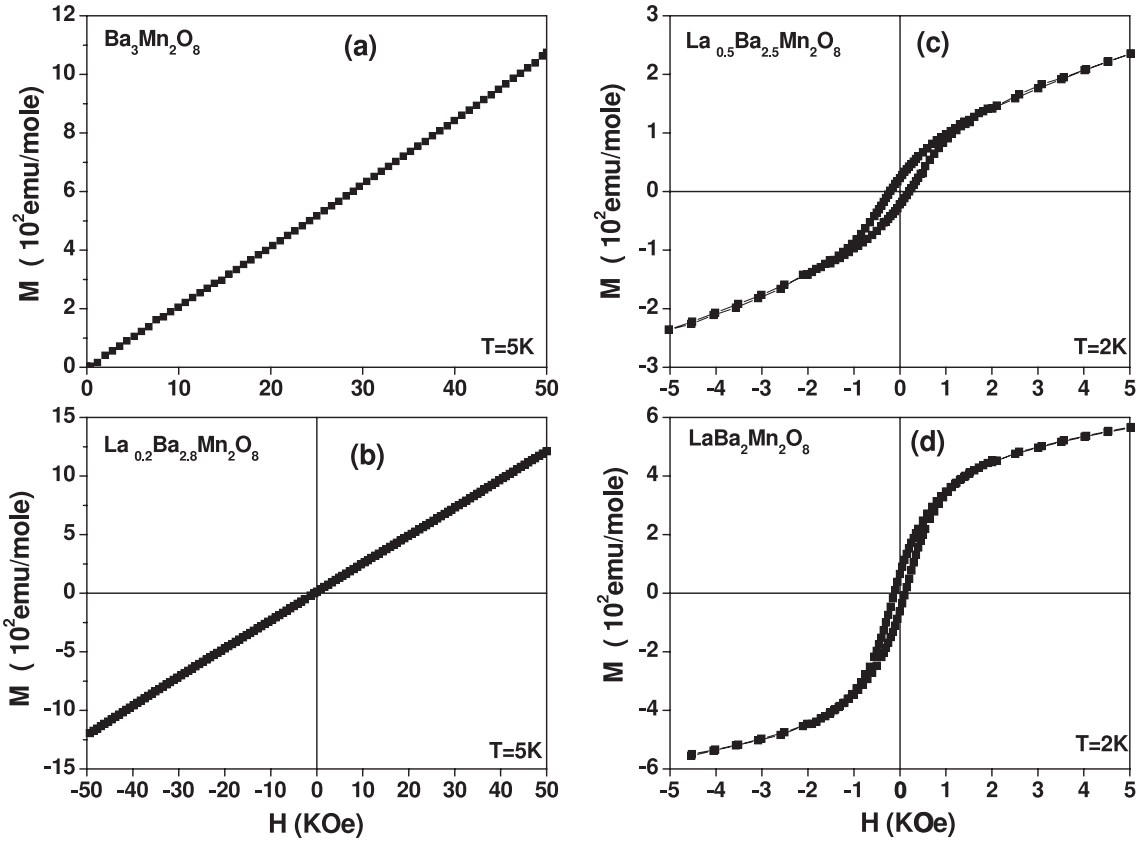

Figure 3. Magnetization (M) versus magnetic field (H) curve at 2 and 5 K for $La_xBa_{3-x}Mn_2O_8$ ($x = 0$, 0.2, 0.5, 1).

interactions, the susceptibility can be expressed as [16]

$$\chi = \frac{\chi_0}{1 + \lambda\chi_0} \tag{2}$$

where $\lambda = 3[J_1+2(J_2+J_3)]/Ng^2\mu_B^2$. The exchange constants J_1, J_2 and J_3 are the second, third and fourth nearest neighbor exchange constants. Very good fits of $\chi(T)$ have been achieved by expression (2) for $x = 0$ and 0.2. The best fitted values of J_0 are 7.7 K and $J_1 + 2(J_2 + J_3) = 5.75$ K which are close to earlier reported values for an undoped ($x = 0$) system [13]. The calculated values of J_0 and $J_1 + 2(J_2 + J_3)$ are 6.9 K and 5.08 K for $x = 0.2$. Temperature dependent susceptibility for $x = 0.5$ and 1.0 cannot be explained by the standard spin dimer model.

Figures 3(a) and (b) reveal that magnetization (M) at 5 K varies linearly with magnetic field (H) up to 5 T for the pure $Ba_3Mn_2O_8$ and $x = 0.2$ compound. The M versus H curve at 2 K below the spin gap transition is shown in figures 3(c) and (d) for $x = 0.5$ and the highest La ($x = 1.0$) doped compound. Hysteresis loops for both compositions, $x = 0.5$ and 1.0 suggest the existence of long range ferromagnetic order for higher concentrations of La. The coercive field (H_c) at 2 K is 115 Oe and remnant magnetization is 65 emu mol^{-1} for $x = 1.0$. The variation of M with H at 300 K for $x = 1.0$, as depicted in figure 4, shows an initial sharp rise to about 35 emu mol^{-1} at 504 Oe and it becomes linear up to a maximum field of 10 kOe. Such M–H behavior indicates a weak ferromagnetic phase at 300 K. In certain spin dimer

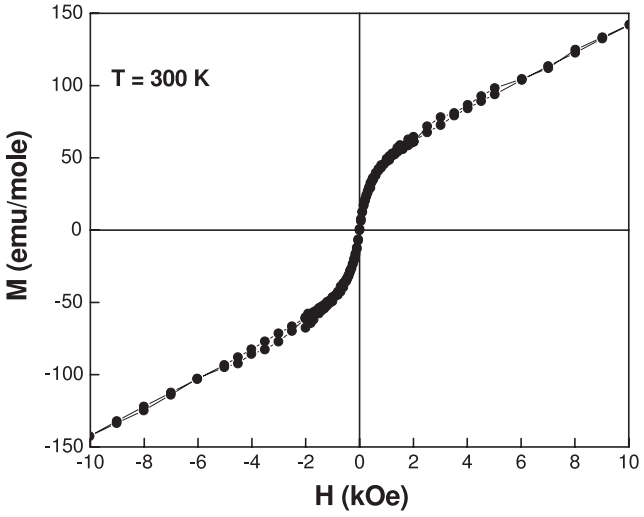

Figure 4. Magnetization (M) versus magnetic field (H) curve at 300 K for $LaBa_2Mn_2O_8$.

compounds, the M–H curve exhibits plateaus at high magnetic field [23]. The coercive field (H_c) at 2 K is 115 Oe and remnant magnetization data do not show any plateaus up to 5 T. The behaviors of $\chi(T)$ and $M(H)$ establish that the short range spin dimer and long range ferromagnetic phase coexist in the La ($x = 0.5$ and 1.0) doped compound. The coexistence of spin dimerization and long range magnetic order was also

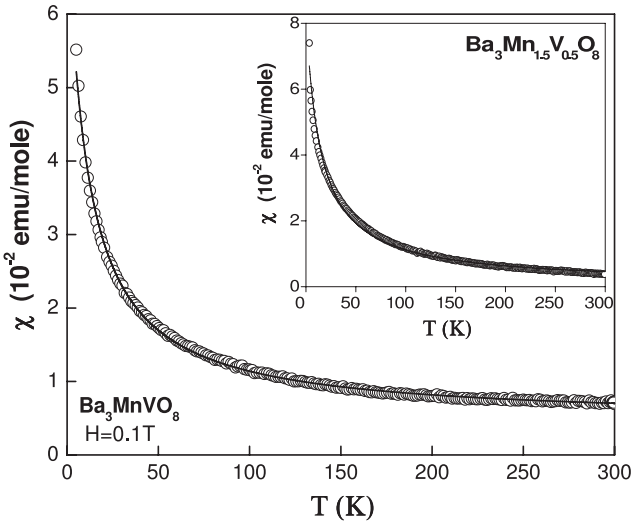

Figure 5. Temperature dependence of magnetic susceptibility for Ba_3MnVO_8 measured under 0.1 T. The open circle and solid line show raw and fitted data, respectively. The inset shows values for $Ba_3Mn_{0.5}V_{1.5}O_8$.

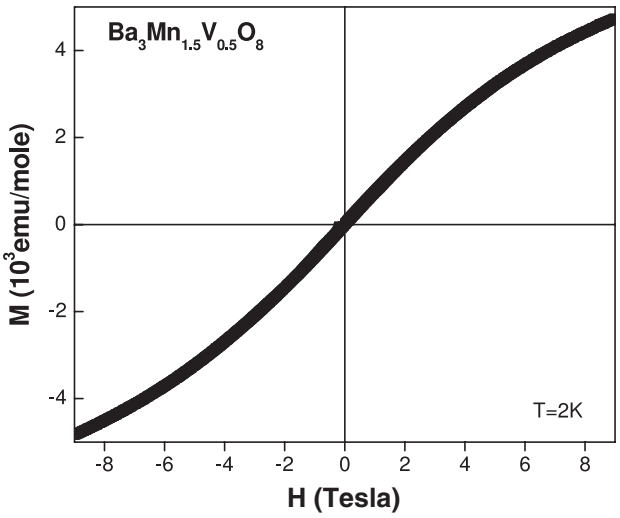

Figure 6. Magnetization (M) versus magnetic field (H) curve at 2 K for $Ba_3Mn_{0.5}V_{1.5}O_8$.

observed in a doped spin-Peierls system [24, 25] $CuGeO_3$, a frustrated spin chain material [26] $LiCu_2O_2$ and a hole doped chain compound [27] $Sr_{0.73}CuO_2$.

The Mn ions reside within MnO_4 tetrahedra separated by Ba–O polyhedra and form double-layered triangular lattices in the basal plane along the c axis. The spin–spin exchange interaction between Mn ions depends on the distance between adjacent MnO_4 tetrahedra. The ionic radius of La^{3+} is 1.27 Å and 1.36 Å for coordination numbers 10 and 12 respectively [28]. The corresponding values for Ba^{2+} are 1.52 and 1.61 Å. Thus the distance between MnO_4 tetrahedra decreases which enhances the magnetic exchange interaction.

In a tetrahedral crystal field, energy levels of the d orbital of transition metal ions are split into e_g and t_{2g} states. The electronic configuration of the Mn^{5+} (d^2) ion is e_g^2. Substitution of La^{3+} for Ba^{2+} induces the mixed valence state, Mn^{5+} and Mn^{4+} for the charge neutrality. Koo *et al* [29] from tight binding electronic structure calculations predicted that the antiferromagnetic spin–spin exchange interaction (J_{AFM}) depends on the occupation of the d orbital. The generation of Mn^{4+} with d^3 configuration clearly affects J_{AFM} which modifies the spin excitation spectrum of $Ba_3Mn_2O_8$. Double exchange interaction takes place between Mn^{5+}–O–Mn^{4+} through intervening oxygen [30]. The spin singlet–triplet dispersion obtained from single crystal inelastic neutron scattering measurements indicates that inter-bilayer interactions play important roles [21]. The nearest and next nearest inter-bilayer interactions are ferromagnetic. Doping of La may enhance inter-bilayer ferromagnetic exchange coupling. Thus the combined effects of double exchange and inter-bilayer ferromagnetic interactions give rise to long range ferromagnetic order for higher La doped systems.

Variation of susceptibility with temperature for V doped samples is displayed in figure 5 for $y = 0.5$ and 1.0. The continuous increase of susceptibility with decrease of temperature clearly suggests the absence of a spin gap transition up to 2 K. The $\chi(T)$ in the entire temperature range is fitted well to the Curie–Weiss law, $\chi(T) = C/(T-\theta) + \chi_0$ for both the compositions. The values of the temperature independent term χ_0 are 7.6×10^{-4} emu mol^{-1} and 4.6×10^{-3} emu mol^{-1} for $y = 0.5$ and 1.0 respectively. The negative values of θ (-14.68 K, $y = 0.5$ and -10.41 K, $y = 1.0$) suggest antiferromagnetic spin correlation for both compositions. The evaluated effective magnetic moment per Mn ion obtained from the best fitted parameter C is 2.18 μ_B and 1.71 μ_B for $y = 0.5$ and 1.0 respectively. Magnetic moments are smaller than 2.82 μ_B for pure compound. It has been found that $Ba_3V_2O_8$ is diamagnetic having magnetic moment -1.346×10^{-2} emu mol^{-1}. The variation of magnetization with magnetic field at 2 K is shown in figure 6. A nonlinear behavior is found up to the maximum field of 9 T.

The highest oxidation state of vanadium is V^{5+} with an empty d^0 orbital. As a result of this, the V^{5+} ion does not possess any magnetic moment. In vanadium doped $Ba_3Mn_2O_8$, Mn^{5+} is replaced by the V^{5+} state due to the nearly equal ionic radius of Mn^{5+} (0.33 Å) and V^{5+} (0.35 Å) in a tetrahedral environment. Hence the substitution of V^{5+} for Mn^{5+} reduces the magnetic moment. The introduction of V impurities breaks the magnetic exchange link among Mn ions. The doping of non-magnetic V weakens the formation of an antiferromagnetically coupled spin dimer.

4. Conclusion

The ground state of the spin dimer compound $Ba_3Mn_2O_8$ is significantly modified by the replacement of divalent Ba by a trivalent La ion. The formation of a mixed valency of Mn ion and ferromagnetic inter-bilayer exchange coupling stabilize the ferromagnetic spin order. The substitution of non-magnetic V at Mn sites completely destroys the spin gap transition. Interplay among intradimer antiferromagnetic exchange, inter-bilayer ferromagnetic and double exchange effects determines

the magnetic properties of an La doped mixed valence dimer $Ba_3Mn_2O_8$ system.

Acknowledgment

This work is funded by the Department of Science and Technology, Government of India (project no. SR/FTP/PS-23/2006).

References

[1] Hase M, Terasaki I and Uchinokura K 1993 *Phys. Rev. Lett.* **70** 3651
[2] Dagotto E and Rice T M 1996 *Science* **271** 618
[3] Ramirez A P 1994 *Annu. Rev. Mater. Sci.* **24** 453
[4] Bose I and Gyan S 1999 *J. Phys.: Condens. Matter* **11** 6427
[5] Haldane F D M 1983 *Phys. Rev. Lett.* **50** 1153
[6] Whangbo M H, Koo H J and Dai D 2003 *J. Solid State Chem.* **176** 417
[7] Whangbo M H, Dai D and Koo H J 2005 *Solid State Sci.* **7** 827
[8] Nikuni T, Oshikawa M, Oosawa A and Tanaka H 2000 *Phys. Rev. Lett.* **84** 5868
[9] Oosawa A, Ishii M and Tanaka H 1999 *J. Phys.: Condens. Matter* **11** 265
[10] Ruegg Ch, Cavadini N, Furrer A, Gudel H-U, Kramer K, Mutka H, Wildes A, Habicht K and Vorderwisch P 2003 *Nature* **423** 62
[11] Sasago Y, Uchinokura K, Zheludev A and Shirane G 1997 *Phys. Rev.* B **55** 8357
[12] Sebastian S E, Harrison N, Batista C D, Balicas L, Jaime M, Sharma P A, Kawashima N and Fisher I R 2006 *Nature* **441** 617
[13] Uchida M, Tanaka H, Bartashevich M I and Goto T 2001 *J. Phys. Soc. Japan* **70** 1790
[14] Nakajima T, Mitamura H and Ueda Y 2006 *J. Phys. Soc. Japan* **75** 054706
[15] Singh Y and Johnston D C 2007 *Phys. Rev.* B **76** 012407
[16] Uchida M, Tanaka H, Mitamura H, Ishikawa F and Goto T 2002 *Phys. Rev.* B **66** 054429
[17] Tsujii H, Andraka B, Uchida M, Tanka H and Takano Y 2005 *Phys. Rev.* B **72** 214434
[18] Stone M B, Lumsden M D, Qiu Y, Samulon E C, Batista C D and Fisher I R 2008 *Phys. Rev.* B **77** 134406
[19] Xu B, Wang H-T and Wang Y 2008 *Phys. Rev.* B **77** 014401
[20] Weller M T and Skinner S J 1999 *Acta Crystallogr.* C **55** 154
[21] Stone M B, Lumsden M D, Chang S, Samulon E C, Batista C D and Fisher I R 2008 *Phys. Rev. Lett.* **100** 237201
[22] Bleaney B and Bowers K D 1952 *Proc. R. Soc.* A **214** 451
[23] Ono T, Tanka H, Kolomiyets O, Mitamura H, Goto T, Nakajima K, Osawa A, Koike Y, Kakurai K, Klenke J, Smeibidle P and Meißner M 2004 *J. Phys.: Condens. Matter* **16** S773
[24] Hase M 1998 *J. Magn. Magn. Mater.* **177** 611
[25] Manabe K, Ishimoto H, Koide N, Sasago Y and Uchinokura K 1998 *Phys. Rev.* B **58** R575
[26] Choi K Y, Zvyagin S A, Cao G and Lemmens P 2004 *Phys. Rev.* B **69** 104421
[27] Meijer G I, Eccleston R S, Mutka H, Rossel C, Karpinski J, Kazakov S and Watchter P 1999 *Phys. Rev.* B **60** 9260
[28] Shannon R D 1976 *Acta Crystallogr.* A **32** 751
[29] Koo H J, Lee K S and Whangbo M H 2006 *Inorg. Chem.* **45** 10743
[30] Zener C 1951 *Phys. Rev.* **82** 403